The Canadian Mineralogist
Vol. 42, pp. 1523-1539 (2004)

THE LENED EMERALD PROSPECT, NORTHWEST TERRITORIES, CANADA: INSIGHTS FROM FLUID INCLUSIONS AND STABLE ISOTOPES, WITH IMPLICATONS FOR NORTHERN CORDILLERAN EMERALD

Daniel D. MARSHALL§

Department of Earth Sciences, Simon Fraser University, Burnaby, British Columbia V5A 1S6, Canada

Lee A. GROAT

Department of Earth and Ocean Sciences, University of British Columbia, Vancouver, British Columbia V6T 1Z4, Canada

Hendrik FALCK

C.S. Lord Northern Geoscience Centre, Yellowknife, Northwest Territories X1A 2R3, Canada

Gaston GIULIANI

IRD and Centre de Recherches Pétrographiques et Géochimiques – CNRS, UPR 2300, 15, rue Notre Dame des Pauvres, BP 20, F–54501 Vandœuvre-lès-Nancy Cedex, France

Heather NEUFELD

Department of Earth and Ocean Sciences, University of British Columbia, Vancouver, British Columbia V6T 1Z4, Canada

Abstract

Vanadium-rich emerald at the Lened occurrence, Northwest Territories, is hosted within a fractured garnet–diopside skarn. The emerald is generally found in quartz–carbonate veins with mm-scale alteration haloes of muscovite and carbonate. The skarn is hosted within the Cambro-Ordovican Rabbitkettle Formation, which overlies black shales of the Devonian Earn Group. Skarn and subsequent quartz–carbonate veins are the result of contact metamorphism related to the emplacement of the adjacent 93 Ma Lened pluton of the Selwyn Plutonic Suite. Fluid-inclusion studies reveal the presence of two distinct fluids, a CO_2-bearing fluid related to emerald precipitation and a brine limited to subsequent crystallization of quartz. The CO_2-bearing fluid is dominantly a dilute aqueous brine with approximately 4.5 mole % CO_2 and minor amounts of CH_4, N_2, and H_2S. The pressure of formation is limited by estimates of the maximum lithostat to less than 320 MPa. The temperatures of formation, in the interval 200–610°C, are constrained by temperatures of fluid-inclusion homogenization and isochore intersections with the 320 MPa maximum lithostatic pressure. Preliminary stable isotope data from Lened are consistent with isotopic data for fluids originating from other nearby plutons of the Selwyn Plutonic suite, indicating that emerald at Lened may be derived from a magmatic source. Geological constraints are consistent with Lened being a Type-I (igneous-activity-related) occurrence of emerald. Oxygen isotope data, fluid compositions, pressures and temperatures of formation similar to those of the Regal Ridge occurrence in the Yukon suggest that emerald in the northern Cordillera is likely igneous-activity-related, although the Regal Ridge and Lened occurrences do display some characteristics of schist-type occurrences as well.

Keywords: Lened prospect, emerald, fluid inclusions, stable isotopes, geochemistry, Northwest Territories.

Sommaire

L'indice d'émeraude riche en vanadium de Lened, dans les Territoires du Nord-Ouest, se trouve dans un skarn à grenat + diopside fracturé. Les cristaux se présentent généralement dans des veines à quartz + carbonate entourées d'un liseré d'altération à muscovite + carbonate. Le skarn s'est développé aux dépens d'un hôte cambro-ordovicien de la Formation Rabbitkettle, qui recouvre les shales noirs dévoniens du Groupe de Earn. Le skarn et les veines à quartz + carbonate sont le résultat du métamorphisme de contact lié à la mise en place du pluton de Lened (93 Ma), de la suite plutonique de Selwyn. Les inclusions

§ *E-mail address*: marshall@sfu.ca

fluides révèlent la présence de deux fluides distincts, un à CO_2 lié à la précipitation de l'émeraude, et une saumure piégée par le quartz seulement, considéré tardif. Le fluide à CO_2 est en grande partie une solution aqueuse diluée de saumure, avec environ 4.5% (base molaire) de CO_2 et des quantités mineures de CH_4, N_2, et H_2S. La pression de formation est délimitée par les estimés de l'épaisseur des roches à moins de 320 MPa. La température de formation, entre 200 et 610°C, environ, est indiquée par la température d'homogénéisation des inclusion fluides et par les intersections des isochores avec la pression lithostatique maximale de 320 MPa. Les données préliminaires sur les isotopes stables à Lened sont conformes aux données isotopiques sur les fluides émanant des plutons avoisinants de la suite de Selwyn. L'émeraude de Lened pourrait donc avoir une dérivation magmatique; d'ailleurs, les contraintes géologiques concordent avec un lien magmatique. Les données sur les isotopes d'oxygène, la composition des fluides, la pression et la température de formation, semblables à celles de l'indice Regal Ridge, au Yukon, font penser que l'émeraude dans les Cordillères du nord auraient une filiation magmatique, quoique les indices de Regal Ridge et Lened possèdent aussi des caractéristiques de gisements mis en place dans des schistes.

(Traduit par la Rédaction)

Mots-clés: indice de Lened, émeraude, inclusions fluides, isotopes stables, géochimie, Territoires du Nord-Ouest.

Introduction

The recent discovery of emerald in the Yukon (Groat *et al.* 2002) has led to increased interest in the Canadian Cordilleran as a source of gem-quality green beryl. Emerald was discovered in skarn at the Lened property in 1997. The property is located north of the Yukon – Northwest Territories border (Fig. 1), 55 km northwest of the town of Tungsten in the Logan Mountains (NTS 105I/7). Geological work in the area includes regional-scale mapping by Green & Roddick (1961) and Blusson *et al.* (1968). More detailed work was carried out by Walton (1997), Gordey & Anderson (1993), Glover & Burson (1987), and Dawson & Dick (1978).

The process leading to the formation of emerald remains poorly understood. The emerald-green color results from the presence of Cr and V (Sinkankas 1981). Emerald results from the existence of unusual geological environments where there is a sufficient abundance of Cr (or V, or both) coupled with a sufficient abundance of Be. Recent studies of a number of emerald deposits worldwide (Schwarz & Giuliani 2001, Banks *et al.* 2000, Vapnik & Moroz 2000, Grundmann & Morteani 1989, Ottaway *et al*. 1994) indicate three main modes of origin for emerald mineralization. Type-I (or granite-related) emerald mineralization is typified by the intrusion of granitic rocks into Cr- or V-bearing host-rocks. In this scenario, the granitic rocks are responsible

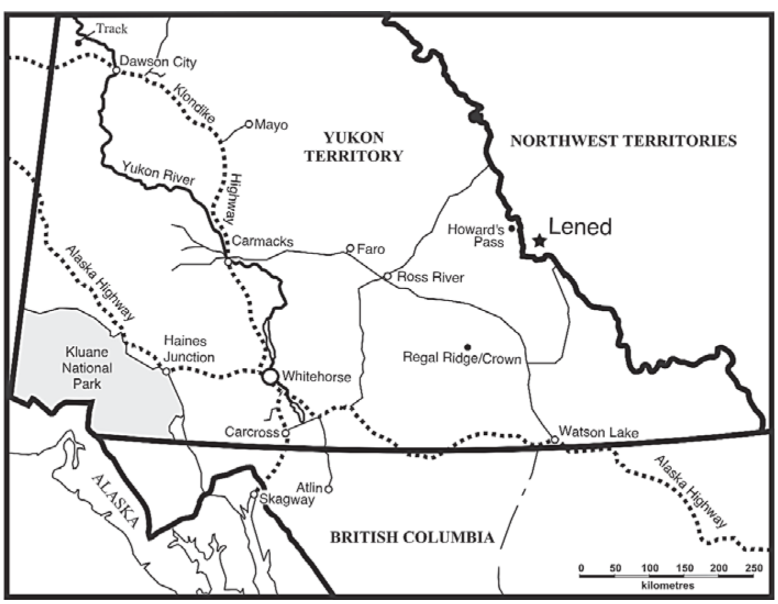

FIG. 1. Index map of the Lened emerald occurrence in the Canadian Cordillera.

for the introduction of heat and Be into the system. Type-II (metamorphic) emerald is typically found in schists of upper greenschist to lower amphibolite grade in tectonically active areas. Emerald formed in this environment results from Be-rich fluids traveling along major crustal breaks such as shears or faults and encountering Cr- or V-rich metamorphic rocks. The heat for Type-II emerald is considered to be the result of regional metamorphism in tectonically active orogens. A third process, leading to a subtype of the second group (Type-IIb emerald), is derived from the interaction of organic-matter-rich shales and highly saline brines derived from evaporites. Beryllium, chromium, and vanadium are released into the fluid phase by a series of self-sustaining, endothermic, sulfate-reducing chemical reactions initiated during regional metamorphism.

Initial genetic studies on Cordilleran emerald from the Regal Ridge property in the Yukon (Groat *et al.* 2002, Marshall *et al.* 2003) provide data that are compatible with the Type-I and Type-II modes of formation. The Regal Ridge showing (Fig. 1) is hosted in Cr- and V-bearing mafic rocks intruded by Cretaceous granitic rocks. These rocks, which are part of the Yukon Tanana terrane, were deformed during the Cretaceous and are close to the Tintina Fault, a major break in the crust. The Lened showing, which is hosted within rocks of the Selwyn basin, was chosen as a suitable area to distinguish between a Type-I and Type-II genesis, as it also is hosted within V- and Cr-bearing rocks in general proximity to Cretaceous granitic rocks, but has experienced less deformation, a lower grade of metamorphism, and there are no major crustal breaks in the vicinity. Fluid-inclusion studies, stable isotope analyses, emerald geochemistry, and petrographic studies of vein material were initiated to determine if both deposits had similar fluid and pressure–temperature histories.

Regional Geology

In the vicinity of the Lened showing (Fig. 2), the clastic sedimentary rocks range in age from Cambrian to Cretaceous (Gordey & Anderson 1993). The oldest unit in the vicinity of the showing is the Upper Proterozoic to Lower Cambrian Vampire Formation, a rusty weathering phyllitic shale. It is grey on fresh surfaces and locally calcareous. Overlying the Vampire Formation is the Cambro-Ordovician Rabbitkettle Formation, which hosts the emerald-bearing quartz–carbonate veins. The Rabbitkettle Formation is generally a dolomitic limestone. It comprises whitish grey dolomitic limestone to dark grey calcareous shaley siltstones, with the siltstone layers attaining a few mm in thickness. Black shales and black cherty siltstones of the Portrait Lake Formation (Earn Group) overlie the Rabbitkettle Formation in thrust fault contact. The Portrait Lake rocks are fine-grained and weather a rusty brown color. Locally, the rocks are cut by many minor faults and thrusts and bedding generally trends northeast-southwest. Folding on the scale of a few hundred meters can be observed in the valley walls.

The sedimentary rocks are intruded by two main phases of a Cretaceous granitic pluton (Fig. 2). The first is a seriate-textured biotite quartz monzonite (Glover & Burson 1987). The second phase is similar to the first, but has K-feldspar phenocrysts attaining a few cm in length. The Lened pluton is approximately 7 km long and 4 km wide. It may be connected at depth to the nearby Rudy and Cac plutons, and this would extend the pluton length to approximately 17 km. No pegmatitic phases have been identified associated with the plutons. However, dikes and small apophyses of the granitic rocks can be found to the southeast of the emerald showing. These plutons contain "two-mica" granitic rocks that have been dated at 93 ± 1 Ma using the K–Ar method on biotite (Gordey & Anderson 1993). The granitic rocks are slightly foliated near the pluton margins. Accessory minerals are muscovite, garnet, andalusite, and tourmaline. The euhedral, inclusion-free, "early-formed" andalusite and garnet are generally found near the pluton margins and have been interpreted as igneous (Gordey & Anderson 1993).

The regional metamorphic grade attained in the local strata is subgreenschist grade. Maximum regional pressures within the map area are estimated, by burial depths and tectonic loads, at 320 MPa (Gordey & Anderson 1993). Contact-metamorphic aureoles are comprised of garnet – diopside ± pyrite skarn in the calcareous rocks and hornfels in the pelitic shales. The aureoles around the granitic rocks are estimated to extend to approximately 1 km from the granitic rocks, with metamorphic andalusite occurring within 500 m of the granitic rocks (Gordey & Anderson 1993). Garnet – vesuvianite – diopside assemblages in the Rabbitkettle carbonates and hornfels developed in the shales of the Earn Group near the showing are also interpreted to be the result of contact metamorphism. In additional, large splays (~10 cm) of tremolite needles are observed near apophyses of the granitic rock elsewhere in the study area.

Vein Petrology

Emerald at the Lened showing is found in quartz–carbonate veins (Fig. 3). The veins strike east–west and have moderate to steep southerly dips. The veins consist predominantly of quartz, with lesser amounts of calcite. The quartz ranges from massive to euhedral, with crystals attaining 3 cm in length. The veins attain 50 cm in thickness. Approximately 45% of the veins contain beryl or emerald. Beryl is abundant in some parts of the vein, comprising up to 10% in areas of 10 cm^3. The crystals of beryl and emerald are idiomorphic and attain lengths of 2.5 cm. Muscovite is common near the vein margins and in the alteration halo (Fig. 4). The

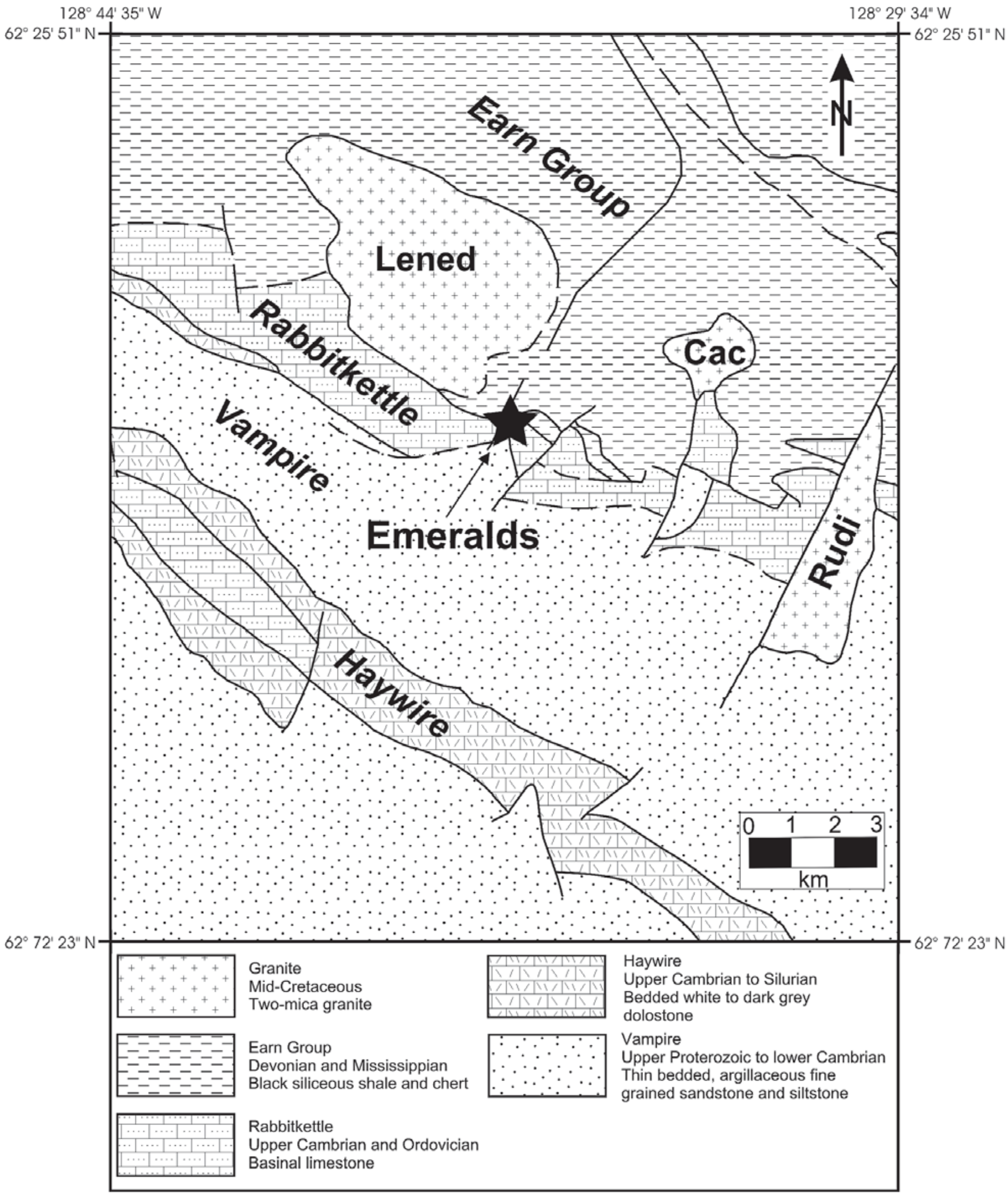

FIG. 2. Geological map of the area of the Lened emerald occurrence, showing the major rock-units within the area (after Gordey & Makepeace 1999).

alteration haloes generally do not extend more than a cm from the vein margin. Muscovite, calcite, garnet and diopside are the dominant minerals in these haloes.

Some veins cut older veins, indicating that there has been more than one generation of fracturing. Some veins contain idiomorphic quartz crystals that overgrow emerald. At least one emerald specimen shows two distinct zones of emerald formation (Fig. 5), suggesting more than one episode of emerald formation. Emerald occurs exclusively within the veins. The color of the emerald is variable, from almost clear to a dark grassy green. The emerald contains abundant inclusions of minerals and fluid. In general, there are fractures perpendicular to the *c* axis of the crystals, and the largest specimen of gem-quality material found is approximately 1 cm in length.

The veins are generally hosted in the contact-metamorphosed calc-silicate rocks of the Rabbitkettle Formation, but do cut the hornfels developed at the expense of the Earn Group shale and unmetamorphosed Rabbitkettle limestone. Thus the veins postdate the calc-silicate skarn or more likely represent the waning stages of skarn formation in a relatively active tectonic regime. Field relationships indicate that the Rabbitkettle limestone has been thrust over the younger Earn Group shales (Fig. 3) and that thrusting is broadly coeval with skarn development.

Composition of the Emerald

Emerald crystals from Lened are typically euhedral, up to 2.5 cm in size, transparent and pale green to yellow in color. Most of the crystals contain inclusions and fractures. Two crystals of emerald were selected for electron-microprobe and LAM–ICP–MS (laser-ablation microprobe – inductively coupled plasma – mass spectrometry) analyses. Five points on each sample were sampled with the electron microprobe, and one point from each crystal was sampled with the laser-ablation microprobe. The analytical resuts were recalculated on the basis of 18 O and 3 Be atoms per formula unit (*apfu*). It is important to note that this approach gives the maximum possible Be content and ignores possible substitution at the Be site. The average compositions are given in Table 1. The average V and Cr contents of the crystals are 1444 and 830, and 14 and 8 ppm, respectively. Both V and Cr are chromophoric in emerald; however, the analyses confirm that V is responsible for the green color in the Lened samples. The elements responsible for most of the variation in color in the Lened and Regal Ridge (Yukon) samples are plotted as oxides in Figure 6a, and corresponding values for emerald from other deposits are shown in Figure 6b. In most cases, the Cr content of an emerald crystal is much greater than that of V; the only consistent exceptions are the samples from Lened. A few of the emerald crystals from Pakistan and Muzo (Columbia) plot near the Lened samples. A comprehensive study of the chemical composition of the Lened emerald, based on numerous samples collected during the summer of 2002, is under way.

Fluid Inclusions

Fluid inclusions in quartz and emerald from Lened are either isolated or occur as planes of inclusions along healed fractures. Despite the presence of growth zones in the emerald, it was not possible to conclusively identify any primary fluid inclusions, as the inclusions do not define the growth zones within the emerald or quartz. There are two fluid-inclusion assemblages (FIAs) at Lened. The most prevalent are carbonic fluid inclusions (Fig. 7, Table 2), found in both quartz and emerald. A rarer FIA of two-phase inclusions of brine (Table 2), found only in quartz, does not contain carbonic phases.

The carbonic inclusions contain three phases at room temperature. The dominant phase is an aqueous brine occupying approximately 75% of the fluid-inclusion volume. The other two phases are gaseous and liquid carbonic fluids, representing approximately 6 and 19% of the volume, respectively. The inclusions generally display consistent phase proportions, suggesting both the trapping of a single-phase, relatively consistent fluid and also the lack of any post-entrapment modification (necking down). These fluid inclusions attain 120 μm and generally display a subrounded to subangular morphology. Most of the inclusions form linear arrays along healed fractures within the host mineral. Some inclusions are isolated and do not appear to have formed along healed fractures.

Upon cooling to –190°C, the three-phase fluid inclusions nucleate three additional phases. On average, clathrate nucleates at approximately –32°C, followed closely by ice nucleation at approximately –47°C; CO_2 freezes at approximately –110°C. When heated from –190°C, the fluid inclusions develop cracks and darken in the range –77 to –65°C. The solid CO_2 in the fluid inclusions in emerald melts over the range –59.1 to –63.5°C (Fig. 8a). This is followed later by the continuous melting of ice, first commencing at an average eutectic of –30°C. The final melting of ice occurs over the temperature range –2.9 to –4.3°C. Clathrate is the next phase to melt, over the temperature interval +8.6 to +10.8°C (Fig. 8b). Homogenization of the carbonic phases occurs over the range +21.3 to +28.7°C. Most of the inclusions undergo homogenization of the carbonic phases to liquid (bubble-point transition), with approximately one third homogenizing to carbonic vapor. Further heating results in total homogenization of the fluid inclusions to liquid over the range 206 to 274°C (Fig. 8c).

The freezing-point depression of CO_2 indicates that the carbonic phases are dominated by CO_2, but contain minor amounts of other dissolved gases. Raman studies on the fluid inclusions hosted within emerald have been ineffective because the emerald host fluoresces, and the

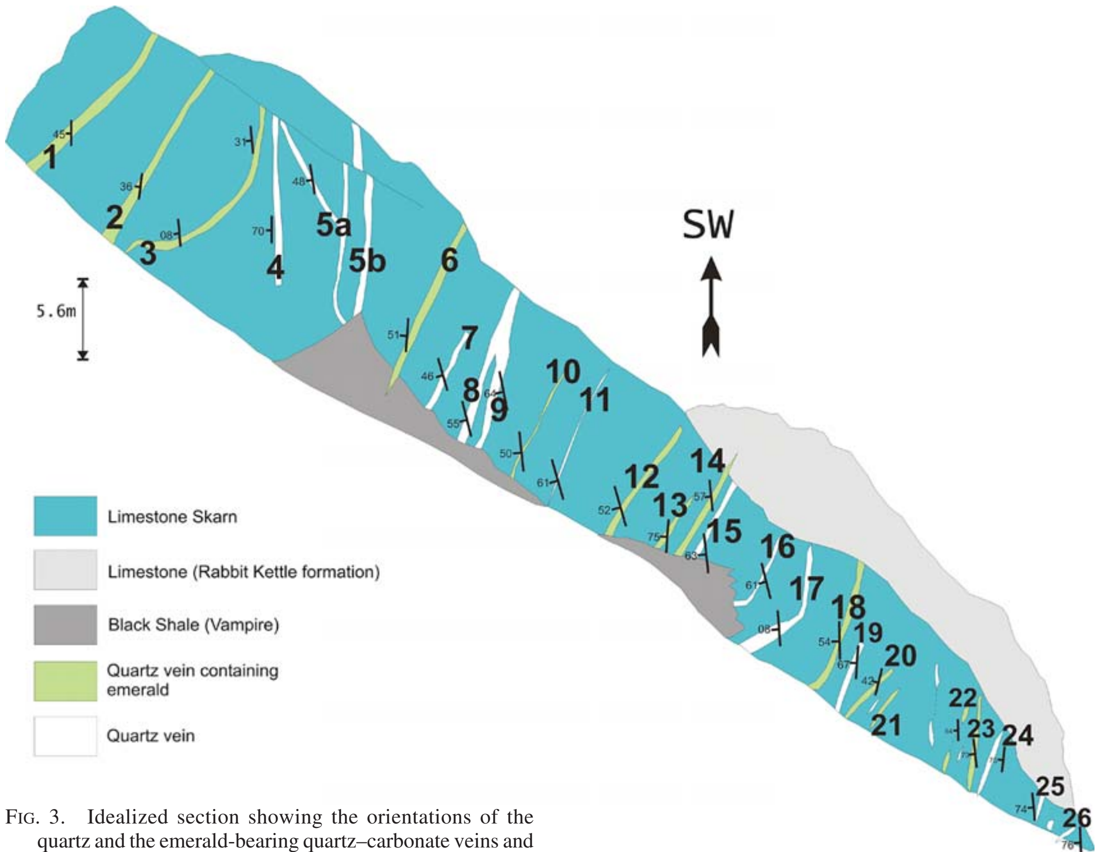

FIG. 3. Idealized section showing the orientations of the quartz and the emerald-bearing quartz–carbonate veins and the cross-cutting relationships to the shale and skarn.

fluorescence overprints any signal from the gases. Raman analyses of fluid inclusions hosted within the quartz are consistent with the presence of N_2, CH_4, and H_2S within the fluid inclusions (Fig. 9). Using the cross-sectional scattering coefficients (Dhamelincourt *et al.* 1979) for CO_2, CH_4, N_2, and H_2S, 1.5, 7.0, 1.0, and 6.4, respectively, and assuming instrumental efficiency-factors of 1.0, we obtained mole fractions of CO_2, CH_4, N_2, and H_2S of 0.985, 0.008, 0.006, and 0.001, respectively.

The complex composition of the gases within the fluid inclusions make salinity determinations difficult. However, the relatively high melting points of clathrate (Table 2) indicate that salinities are low. Assuming that the slight amounts of H_2S and N_2 in the inclusion behave as CH_4 (in terms of the effect on clathrate melting) and extrapolating the data of Diamond (1992), the maximum salinities can be estimated at approximately 2 wt.% NaCl equivalent. To complement the microthermometric determinations of salinity, one grain of emerald and one grain of quartz were frozen in liquid nitrogen, broken and rapidly placed (uncoated) in the

TABLE 1. AVERAGE COMPOSITIONS OF EMERALD FROM THE LENED SHOWING, NORTHWEST TERRITORIES

Sample	1	2		1	2
SiO_2 wt.%	65.06 (0.15)	65.28 (0.22)	Si *apfu*	5.975	5.974
Al_2O_3	17.12 (0.16)	17.46 (0.25)	Al	1.853	1.884
Sc_2O_3	0.03 (0.02)	0.01 (0.02)	Sc	0.002	0.001
V_2O_3	0.29 (0.10)	0.20 (0.10)	V^{3+}	0.021	0.015
BeO*	13.68 (0.02)	13.64 (0.02)	Be	3.000	3.000
MgO	0.93 (0.10)	0.80 (0.16)	Mg	0.128	0.109
FeO	0.38 (0.03)	0.32 (0.07)	Fe^{2+}	0.029	0.024
Na_2O	0.84 (0.08)	0.76 (0.13)	Na	0.150	0.135
K_2O	0.01 (0.01)	0.00 (0.00)	K	0.001	0.000
Cs_2O	0.15 (0.03)	0.08 (0.07)	Cs	0.006	0.003
			Sc ppm	113	244
Total	98.49 (0.09)	98.55 (0.31)	V	1444	830
			Cr	14	8
			Cs	621	1061

Note: For each sample, five point compositions were used in averaging (electron-microprobe data). Compositions were recalculated on the basis of 3 Be and 18 O *apfu*. Standard deviations (1σ) are shown in parentheses. Cr and Ca were sought by electron microprobe but were not detected. The Sc, V, Cr, and Cs ppm values were obtained by LAM–ICP–MS; Ca, Ti, Sr, Ta, W, and REE were sought but not detected. * Determined by stoichiometry.

FIG. 4. Close-up photo showing a quartz vein within the calc-silicate (skarn) host-rock, and the limited muscovite-dominant alteration halo surrounding the vein. Inset photo of emerald in quartz vein with thumb for scale.

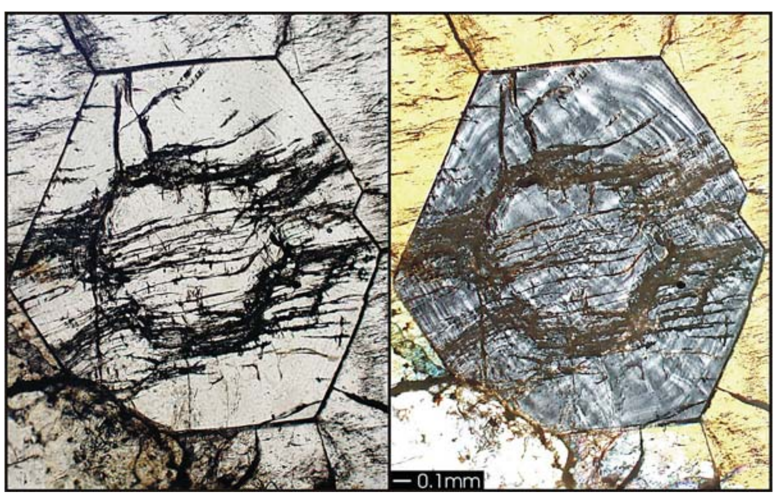

FIG. 5. (a) Photomicrograph of a zoned crystal of emerald in plane-polarized light. Note the two main zones within the emerald. (b) Same photo as a taken under crossed polars. The more cryptic zoning within the inner and outer zones is interpreted to be due to minor amounts of deformation, as no chemical or fluid-inclusion zonation was observed.

TABLE 2. DATA ON FLUID INCLUSIONS IN EMERALD AND QUARTZ FROM THE LENED SHOWING, NORTHWEST TERRITORIES

chip number	T_m CO_2	eutectic	T_m ice	T_m cla	T_h CO_2 [1]	T_h tot	chip number	T_m CO_2	eutectic	T_m ice	T_m cla	T_h CO_2 [1]	T_h tot
Lened 1-1-1	n.v.	n.v.	-3.9	9.8	n.v.	227	DM02-13-3b *		n.v.	-2.8			dec
Lened 1-1-2	-61.4	n.v.	-4.3	10.4	**26.5**	242	DM02-13-3c	-58.2	n.v.	-3	9.7	30	207
Lened 1-1-3	-61.4	n.v.	-3.7	10.6	**25.5**	240	DM02-13-3d	-57.9	n.v.	-3.1	9.4	31	205
Lened 1-1-4	-61.3	n.v.	-4.0	10.8	**24.3**	240	DM02-13-3e	-58.1	n.v.	-3.3	9.3	30	207
Lened 1-1-5	-61.0	-19.0	-4.0	10.5	**26.6**	244	DM02-13-3f	-58.3	n.v.	-3.3	9.3	30	207
Lened 1-1-6	-61.8	n.v.	-3.9	9.9	**25**	227	DM02-13-4a	-58.6	n.v.	-3.2	9.4	29	205
Lened 1-1-7	-62.8	n.v.	-3.4	9.6	**26.8**	236	DM02-13-4b	-57.6	n.v.	-3.5	9.2	29	203
Lened 1-1-8	-62.9	n.v.	-3.9	9.9	**26.7**	238	DM02-13-4c	-58.2	n.v.	-3.4	9.4	29	205
Lened 1-2-9	n.v.	-25.0	-3.9	10.6	**25.2**	214	DM02-13-4d	-58.3	n.v.	-3.2	9.5	29	203
Lened 1-2-10	n.v.	n.v.	-3.9	10.1	n.v.	250	DM02-13-4e	-58.6	n.v.	-3.6	9.2	30	207
Lened 1-2-11	n.v.	n.v.	-3.5	9.6	n.v.	206	DM02-13-4f	-58.9	n.v.	-3.9	9	30	208
Lened 1-2-12	n.v.	n.v.	-3.8	9.4	n.v.	216	DM02-13-5a	-58.7	n.v.	-3.4	9.2	31	193
Lened 1-2-13	n.v.	n.v.	n.v.	10.0	**25.9**	247	DM02-13-5b	-58.5	n.v.	-3.6	9.1	30	210
Lened 1-2-14	n.v.	n.v.	-3.5	9.9	**26.5**	260	DM02-13-5c	-58.7	n.v.	-4.3	8.7	30	215
Lened 1-2-15	n.v.	n.v.	-5.0	9.0	**28.7**	261	DM02-13-5d	-58.4	n.v.	-3.7	9.1	30	210
Lened 1-2-16	-62.4	n.v.	-4.8	9.8	**25.8**		DM02-13-5e	-58.6	n.v.	-4.1	n.v.	30	215
Lened 1-2-17	n.v.	n.v.	n.v.	9.9	**25.5**	265	DM02-13-5f	-58.8	n.v.	-4.3	8.6	30	214
Lened 1-2-18	-63.3	n.v.	n.v.		**21.3**	261	DM02-13-6a	-58	n.v.	-2.9	9.4	n.v.	dec
Lened 1-2-19	n.v.	n.v.	-3.5	10.0	n.v.	259	DM02-13-6b	-58.2	n.v.	n.v.	9.7	23	dec
Lened 1-2-20	-63.5	n.v.	n.v.	9.6	**27.3**	269	DM02-13-6c	-58.1	n.v.	-3.1	10	23	dec
Lened 1-3-21	-59.8	-27	-3.6	9.7	28.7	221	DM02-13-6d	-58	n.v.	n.v.	9.9	22	dec
Lened 1-3-22	-59.4	-27	-3.6	10.1	27.3	211	DM02-13-6e	-57.7	n.v.	-3	9.4	30	dec
Lened 1-3-23	-59.2	-26	-3.3	10.1	28.4	233	DM02-13-6f	-57.9	n.v.	-3	9.8	23	dec
Lened 1-3-24	-59.1	-17	-3.3	9.7	28.7	238	DM02-13-6g	-57.9	n.v.	n.v.	9.5	n.v.	dec
Lened 1-3-25	-59.6	-27	-3.7	10.0	25.8	240	DM02-13-7a	-57.9	n.v.	-3.5	n.v.	n.v.	dec
Lened 1-3-26	-59.2	-44	-3.5	9.9	27.1	216	DM02-13-7b	n.v.	n.v.	-4	8.5	n.v.	206
Lened 1-3-27	-59.6	-40	-3.5	9.6	27.5	239	DM02-13-7c	n.v.	n.v.	-3.7	9.2	n.v.	205
Lened 1-4-28	n.v.	-37	-3.7	9.8	n.v.	219	DM02-13-7d	n.v.	n.v.	-3.3	9.1	n.v.	205
Lened 1-4-29	n.v.	n.v.	-3.9	8.6	n.v.	212	DM02-13-7e	n.v.	n.v.	-3.5	9.1	n.v.	206
Lened 1-4-30	-60.3	-42	-3.9	9.9	25.4	223	DM02-13-7f	n.v.	n.v.	-3.6	9	n.v.	206
DM02-13-1a *		*-28*	*n.v.*			*121*	*DM02-13-8* *		*n.v.*	*-2.7*			*99*
DM02-13-1b *		-28	-2.9			146	*DM02-13-9* *		*n.v.*	*-3*			*149*
DM02-13-1c *		*-26*	*-1*			*138*	DM02-13-10 *		n.v.	-3.3			186
DM02-13-1d *		*-26*	*0*			*130*	DM02-13-11 *		n.v.	-3.3			171
DM02-13-2a	n.v.	n.v.	-3.4	9.5	n.v.	204	DM02-13-12 *		n.v.	-3.2			194
DM02-13-2b	n.v.	n.v.	-3.2	9.3	n.v.	196	DM02-13-13 *		n.v.	-3.3			161
DM02-13-2c	n.v.	n.v.	-3.1	9.4	n.v.	206	DM02-13-14 *		n.v.	-3.4			192
DM02-13-2d	n.v.	n.v.	-3.5	9.1	n.v.	205	DM02-13-15 *		n.v.	-3.3			141
DM02-13-2e	n.v.	n.v.	-3.9	n.v.	n.v.	206	DM02-13-16 *		n.v.	-3.7			195
DM02-13-3a	-58.2	n.v.	-3.1	9.6	30	211							

[1] CO_2 homogenizes into **liquid (in bold)**, CO_2 homogenizes into vapor (normal font). n.v.: not visible. dec: decripitation. DM02 fluid inclusions hosted in quartz. Other inclusions listed are hosted in emerald. Data shown on lines marked with an asterisk are brine inclusions with no CO_2. Data in *italics* are from brine inclusions exhibiting metastable melting of ice.

chamber of a Bausch & Lomb Nanolab scanning electron microscope (SEM) equipped with an energy-dispersion X-ray (EDX) system. The mineral grains were examined using a modified technique after Kelly & Burgio (1983) for breached fluid inclusions. Several cavities resembling breached fluid inclusions were found in the quartz and emerald samples. No residua were visible within or surrounding the fluid-inclusion cavities. The electron beam was directed inside a number of breached inclusions and an EDX spectrum was collected. Likewise, an area encompassing the breached inclusions and the surrounding area was scanned and an EDX spectrum collected. In all cases, the spectra contained the predicted peaks of the host minerals, but no peaks attributable to the major chlorides (Na, K, Mg, Ca, or Cl) were observed, suggesting low-salinity fluids within the frozen inclusions.

Combining the results of measurements of salinity, Raman spectra, phase-volume estimates obtained from flat fluid inclusions, microthermometric observations and the iterative technique of Diamond (2001) for phase-volume determinations, we "estimated" an average fluid-inclusion composition of 0.945 mole % H_2O, 0.046% CO_2, 0.003% CH_4, 0.004% NaCl (~2 wt.% NaCl eq.), 0.001% N_2, and 0.001% H_2S. The bulk molar volume for the "estimated" average fluid inclusion can be approximated using the homogenization of the carbonic phases and the method of Diamond (2001) for the H_2O–CO_2 binary. We deem this method to be the most reliable, as the necessary experimental work in the

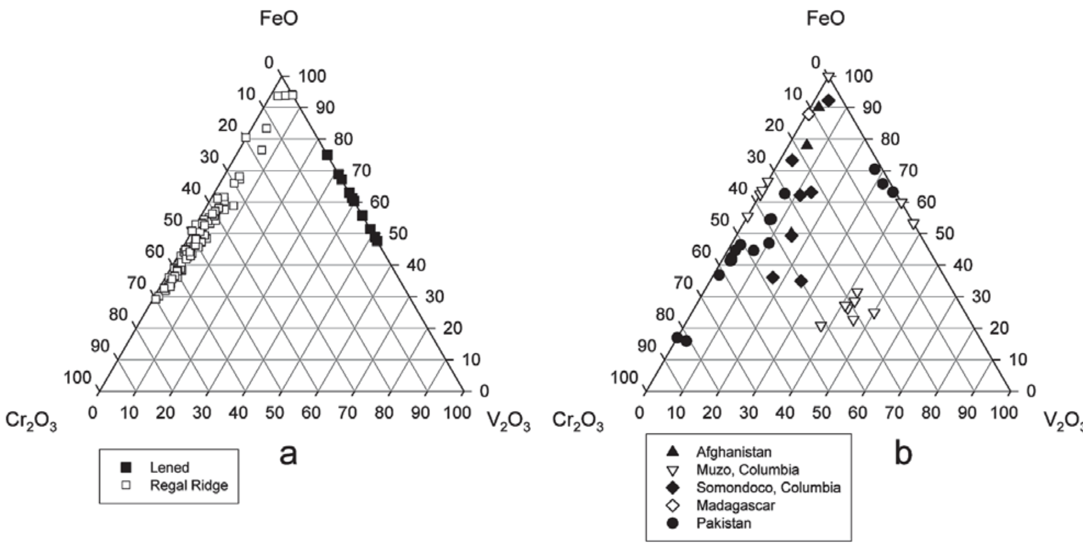

FIG. 6. The composition of emerald plotted in terms of $FeO–Cr_2O_3–V_2O_3$ (weight proportions) from (a) this study, and (b) from the literature (with all Fe as FeO). Sources of data: Kovaloff (1928), Zambonini & Caglioto (1928), Leitmeier (1937), Otero Muñoz & Barriga Villalba (1948), Gübelin (1958), Vlasov & Kutakova (1960), Martin (1962), Petrusenko *et al.* (1966), Beus & Mineev (1972), Hickman (1972), Hanni & Klein (1982), Graziani *et al.* (1983), Kozlowski *et al.* (1988), Hammarstrom (1989), Ottaway (1991), and Groat *et al.* (2002). The diagrams are after Hammarstrom (1989).

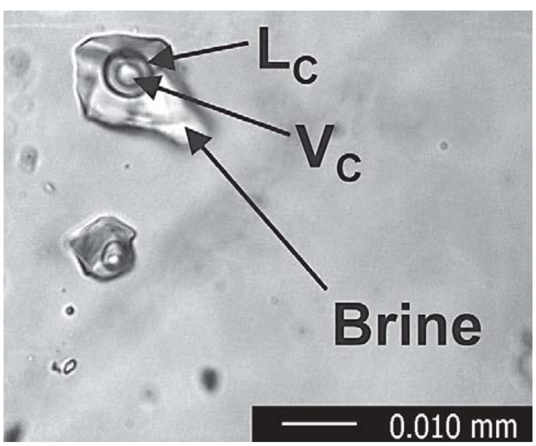

FIG. 7. Photomicrograph of a typical three-phase fluid inclusion in emerald. The three phases observed at room temperature are a brine, a liquid (L_c) and vapor (V_c) carbonic phase. Photo taken in plane-polarized light.

$H_2O–CO_2–NaCl–CH_4–N_2–H_2S$ system has not been done, and CO_2 and H_2O account for over 99 mole % of the fluid. This method yields molar volumes in the range 24.9 and 25.8 cm^3/mole.

The two-phase brine inclusions are comprised of a liquid and a vapor at room temperature. The vapor phase contains no compressible gases and probably contains H_2O vapor only. The liquid phase is a brine and occupies approximately 90% of the fluid-inclusion volume. The inclusions attain 55 μm, with morphologies ranging from subrounded to subangular, with jagged edges. The inclusions occur along healed fractures as linear arrays. None of the inclusions in this FIA could be identified as primary. Cooling the brine inclusions from room temperature to –190°C results in the nucleation of ice at approximately –35°C. Warming the inclusions results in the darkening of the crystals as they are heated to about –70°C, but no melt is visible until approximately –28°C. Further heating results in most of the ice melting over the range –3.7 to –2.9°C (Table 2). Some inclusions display ice melting up to 0°C, but such measurements are not reproducible and are deemed the product of metastable melting of ice (Roedder 1984). Continued heating results in total homogenization over the temperature range 141 to 195°C (Fig. 8c, Table 2). The exact composition of the brines was not determined, thus the salinity is assumed to be due to pure NaCl, and these inclusions thus range from 4.7 to 5.9 wt.% NaCl equivalent. This brine FIA is found only in quartz crystals, and it has generally lower temperatures of homogenization than the carbonic FIA. Quartz samples have been observed that have only the brine FIA. Quartz and

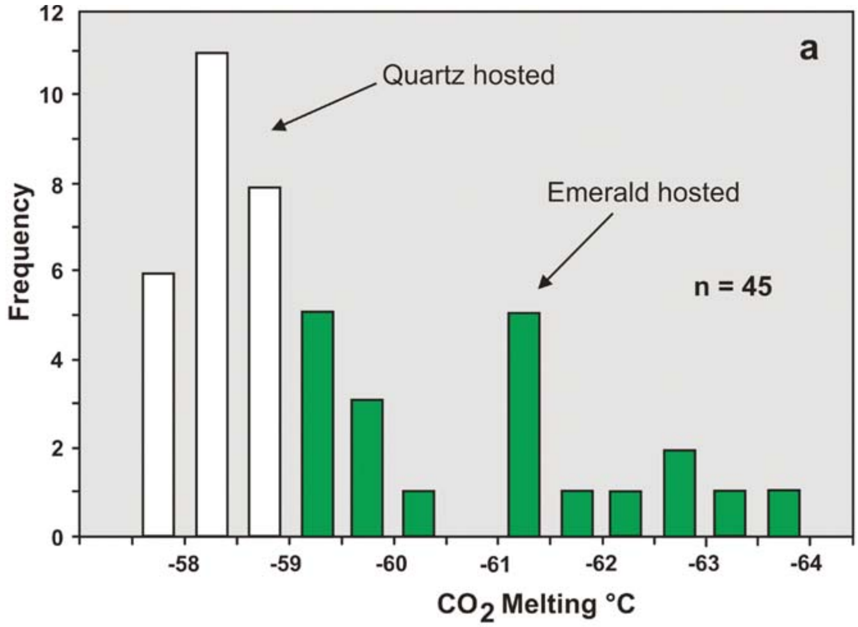

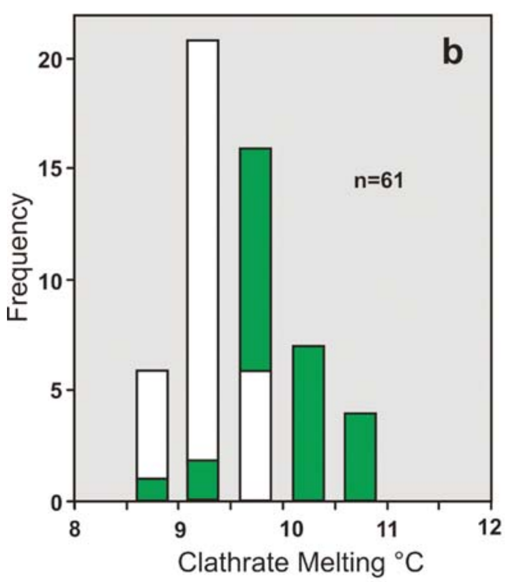

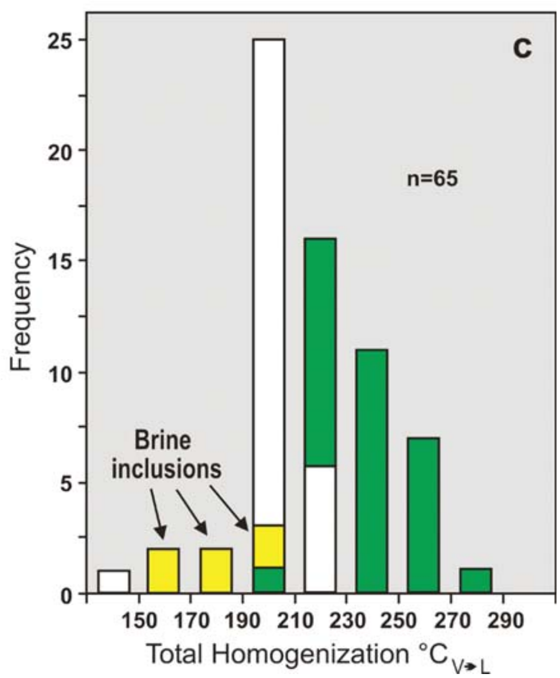

FIG. 8. (a) Histogram of CO_2 melting temperature of carbonic fluid inclusions hosted within quartz (dark grey) and emerald (black). (b) Plot of clathrate melting temperature for carbonic fluid inclusions hosted within emerald and quartz. (c) Histogram showing temperature of total homogenization for inclusions hosted within quartz and emerald, showing a peak in the range 190 to 230°C. Brine fluid inclusions are shown in light grey.

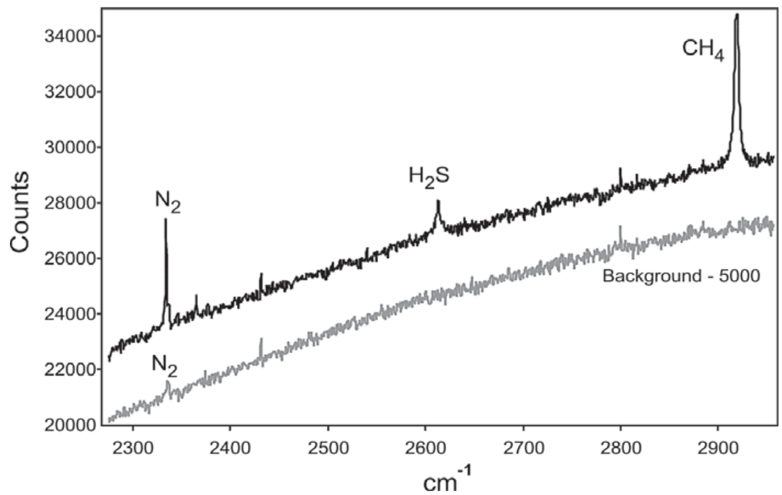

FIG. 9. Raman spectrum showing the N_2, CH_4 and H_2S peaks for a typical three-phase fluid inclusion hosted within quartz (black). A background spectrum for the quartz is shown in dark grey. Note the N_2 peak in the background spectrum, attributed to atmospheric nitrogen. The final results have been corrected for atmospheric nitrogen.

TABLE 3. STABLE-ISOTOPE DATA, EMERALD FROM THE LENED SHOWING, NORTHWEST TERRITORIES

Sample	$\delta^{18}O$ (‰, SMOW)
DM-1a	12.4†
DM-2a (area)	14.05
LG-Lened-1	13.1
LG-Lened-2	12.85

† Average of two analyses.

emerald samples have been observed to contain both the brine and carbonic FIAs in the same host crystals. No samples containing only the carbonic FIA have been observed; thus the brine FIA is interpreted to postdate the carbonic FIA and emerald precipitation.

STABLE ISOTOPES

The oxygen isotopic composition, obtained from seven samples, reveals a range in $\delta^{18}O_{SMOW}$ (Table 3) from 12.4 to 14.05‰. For comparison, these values are shown in grey on Figure 10. There are no data for the δD of the Lened emerald. However, there is good agreement between the $\delta^{18}O$ of Lened and the Regal Ridge (Groat *et al.* 2002) showing, indicating that the two emerald showings may have a similar origin.

PRESSURE–TEMPERATURE CONSTRAINTS

Pressure–temperature (P–T) conditions of vein formation can be obtained by combining the pressure–temperature data from the literature with the fluid-inclusion isochores from this study. Gordey & Anderson (1993) reported a total maximum lithostatic pressure of 320 MPa and the occurrence of metamorphic andalusite in metamorphic haloes and igneous andalusite within the Cac pluton (Fig. 2). Field evidence indicates that the Cac, Rudi, and Lened plutons are similar in texture and composition and may be connected at depth. Thus the presence of andalusite can be used as a constraint on maximum pressure, but as there is some debate as to the exact position of the aluminosilicate triple point (Cesare *et al.* 2003), for the purpose of constraining P–T in this study, a maximum lithostatic pressure of 320 MPa is used. As the Rudi, Cac, and Lened plutons were emplaced at the same depth, the magmatic and metamorphic andalusite provide a second constraint on maximum pressure of 385 MPa for the veins (Fig. 11), and this is consistent with the maximum calculated lithostat. However, the temperature cannot be constrained using the aluminosilicate triple point, as there are several hundred meters of wallrock between the Lened pluton and the emerald veins, and a geothermal gradient between the two. There are no other thermobarometers in the wallrock nor inclusions in the granite that could be used to intersect the kyanite–andalusite or sillimanite–andalusite reaction curves to further constrain P and T.

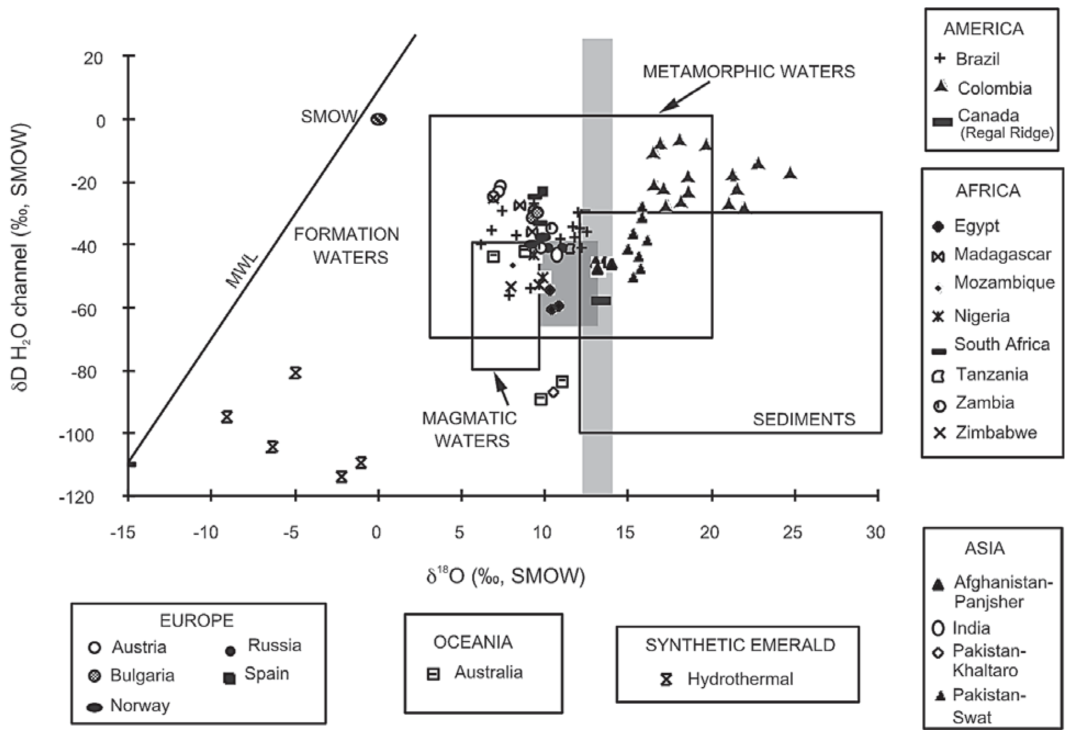

FIG. 10. Channel δD H_2O *versus* calculated $\delta^{18}O$ H_2O (‰, SMOW) for emerald from deposits worldwide (Groat *et al.* 2002, Giuliani *et al.* 1998). The $\delta^{18}O$ range of the Lened emerald is shown in transparent blue. The extended magmatic field for Cornubian (peraluminous) granites is shown in grey. The isotopic compositional fields are from Sheppard (1986).

Fluid-inclusion isochores (Fig. 11) have been derived for both the carbonic and brine FIA. Isochores for the carbonic inclusions were derived using the maximum and minimum constraints from the microthermometry, the GASWET8 program (Bakker 1999), and the modified equation of state for ternary H_2O–CO_2–NaCl fluids (Bowers & Helgeson 1983). Isochores for the brine inclusions were derived using the maximum and minimum constraints from the microthermometry, the FLINCOR program (Brown 1989), and the Zhang & Frantz (1987) equation of state for H_2O–NaCl. Data from fluid inclusions exhibiting metastable melting behavior were not used in the calculation.

The P–T constraints for the carbonic inclusions are defined by the intersection of the minimum isochore and 320 MPa. This occurs at approximately 610°C. Further constraints can be derived from the temperatures of homogenization of the fluid inclusions. The fluid inclusions are consistent with trapping in a one-phase field, indicating that the fluids were not boiling during vein formation. Therefore, the temperature of total homogenization can be used as a minimum temperature constraint. The data (Fig. 8c) exhibit peaks in the 230 to 250°C range, which provides a minimum temperature of formation for the emerald veins. The P–T constraints for the brine inclusions are derived using the same graphical method. This approach yields temperature constraints ranging from approximately 140 to 425°C and pressures of formation ranging up to 320 MPa.

Discussion

We interpret the calc-silicate and hornfels as the products of hot fluids expelled from the cooling Lened pluton, traveling along the thrust fault (Fig. 3). Prolonged emplacement of the pluton, slow cooling and regional tectonic activity resulted in further deformation of the country rocks, with the calc-silicate rocks behaving in brittle fashion, and the unmetamorphosed rocks behaving in a more ductile fashion. This resulted in the creation of a set of subparallel tension fractures in the calc-silicate rocks. These fractures became conduits for hydrothermal fluids emanating from the granitic rocks. Quartz, calcite, emerald, and muscovite were precipitated along these fractures, resulting in a series of subparallel veins (Fig. 3).

We have documented two FIAs. The dominant fluid in both emerald and quartz is represented by carbonic fluid inclusions. The second fluid is represented by two-phase fluid inclusions that are relatively rare and only found in quartz. These two fluids cannot represent the conjugate sets of a boiling system, for the following reasons. (1) The carbonic fluid inclusions have higher temperatures of homogenization than the brine inclusions. (2) The carbonic fluid inclusions are comprised of greater than 95% H_2O; thus if the carbonic fluid inclusions were the result of a boiling system, then there has been remixing of the unmixed fluids to obtain such an elevated percentage of H_2O, and we see no evidence of mixing in the two FIAs. (3) If the FIAs were the conjugates of a boiling system and separated at elevated temperatures, the brine inclusions should have some dissolved CO_2, but no CO_2 was observed in any of the brine inclusions. (4) The carbonic fluid inclusions found in the Lened emerald have very similar compositions to the fluid inclusions found at the Regal Ridge showing in the Yukon (Groat *et al.* 2002), and the better-constrained pressures and temperatures of formation of the emerald there preclude boiling. (5) Isochores (Fig. 11) indicate no overlap for the two FIAs, suggesting that both formed at different P–T conditions and therefore at different times. Therefore, the carbonic fluid is interpreted to have been trapped at a slightly higher metamorphic grade, likely related to the expulsion of fluids from the granite. In addition to the granitic rocks at Regal Ridge, CO_2-rich fluids have been documented at a number of localities in the area, including the Cantung mine (Mathieson & Clark 1984) and the Little Nahanni pegmatites (Marshall *et al.* 2002). The brine fluid is interpreted to be the local metamorphic fluid permeating back into the warm metamorphic aureole after the granite cooled.

Stable isotope data on oxygen and hydrogen from fluid in equilibrium with emerald from a number of deposits worldwide show a great variety of values (Fig. 10). The isotopic data from Regal Ridge plot in the extended magmatic field for peraluminous (Cornubian) granites (Fig. 10). This range of isotopic data is fairly typical of other highly evolved S-type granites of the Selwyn suite (*cf.* Bowman *et al.* 1985). These O and H data also lie within the field typical of metamorphic fluids. In the stable isotope study of the nearby Cantung scheelite skarn, Bowman *et al.* (1985) reported values for the skarn and carbonate host-rocks. The O and H data for the Cantung skarn show very little contribution from the host carbonates and are consistent with fluids typical of peraluminous granites. The oxygen isotope data from the Lened emerald are very similar to the values obtained from the Regal Ridge emerald, which suggests that emerald from Lened and Regal Ridge may have had a similar paragenesis. We interpret the stable isotope data from the Canadian occurrences of emerald as reflecting a genesis similar to the Cantung skarn, and suggest that in the regional context, the stable isotope data are consistent with a magmatic origin.

The major difference between the Regal Ridge and Lened locality is the Cr content of the emerald. Emerald from the Regal Ridge showing is relatively enriched

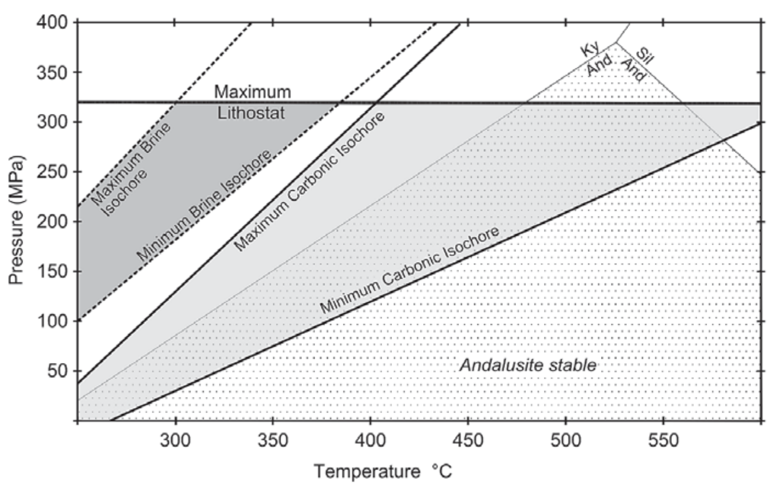

FIG. 11. Pressure–temperature diagram showing the constraints on the formation of emerald veins. The stability field from Holdaway (1971) for andalusite (And) is shown in the stippled pattern. Constraints imposed by the maximum and minimum isochores have been derived from the fluid inclusions. The maximum lithostat value is from Gordey & Anderson (1993). The shaded area shows the range of possible pressure–temperature conditions for emerald precipitation. Symbols: Ky kyanite, Sil sillimanite.

in Cr (Groat *et al*. 2002), whereas the Lened emerald is very rich in V with virtually no Cr. A lack of geochemical data on the host shale and limestone at Lened precludes further discussion, but we believe that these rocks have less Cr than the host mafic and adjacent ultramafic rocks at the Regal Ridge showing.

Our initial reason in studying the Lened emerald was as a potential analogue for the Regal Ridge showing in the Yukon. Systems of genetic classification for emerald deposits around the world indicate that most known emerald deposits fall into two major types (Schwarz & Giuliani 2001). Deposits of Type I are related to granitic intrusions, and those of Type II are associated with metamorphic rocks and large-scale tectonic structures and are not directly related to granitic intrusions. A subset of the Type II (Muzo type) in the eastern Cordillera of Columbia is the result of thermochemical reduction of evaporitic sulfate brines involving organic matter from local black shales (Ottaway *et al.* 1994, Schwarz & Giuliani 2001). The metamorphic grade of the country rocks at Lened is subgreenschist (Gordey & Anderson 1993), and much lower than the middle-greenschist to lower-amphibolite regional metamorphic grade at Regal Ridge. There are no major crustal structures near Lened, and both Lened and Regal Ridge are spatially related to granites of the Selwyn Suite. Thus, Lened is likely to be a Type-I deposit. However, the Lened occurrence does show some similarities with the Muzo subtype. Most notably, Lened is in thrust contact with graphitic shales, but lacks the ubiquitous pyrite found at Muzo (Ottaway *et al.* 1994). The Regal Ridge occurrence has characteristics of type I and II, but has no similarity to the Muzo subtype. Regal Ridge thus is a Type-I emerald occurrence as well, although further study is necessary at both occurrences. There is still the potential for all three types of emerald formation in the Canadian Cordillera.

Conclusions

1) The Lened quartz–carbonate veins are hosted within skarn above a thrust contact with shales of the Earn Group in the vicinity of a 93 Ma S-type (evolved) granite. The veins have mm-scale alteration haloes consisting of muscovite and carbonate.

2) The pressure estimates for emerald formation at the Lened emerald occurrence range from very low pressures to a maximum of 320 MPa. Minimum temperatures based on temperatures of fluid-inclusion homogenization are on the order of 200°C, with maximum temperatures of approximately 610°C obtained from isochore intersections with a 320 MPa maximum in lithostatic pressure. Conditions are not as tightly constrained, but do overlap with the conditions of formation for the Regal Ridge emerald occurrence in the Yukon.

3) There are two distinct FIAs at Lened. A carbonic FIA associated with emerald and a later FIA represented by brine inclusions associated with some of the quartz veins.

4) The carbonic fluid inclusions within the emerald at both Lened and Regal Ridge are almost identical, consisting of approximately 94.5 mole % aqueous brine and 4.5 mole % CO_2, with the remaining 1% composed of CH_4, N_2 and H_2S.

5) Preliminary analyses of the emerald indicate that the Lened emerald is rich in V, with very low concentrations of Cr.

6) Preliminary oxygen isotope analyses are similar to values obtained from the Regal Ridge occurrence.

7) The geological evidence is consistent with the Lened occurrence being related to the nearby Cretaceous granitic rocks, which are the most likely source of Be, with V extracted from the nearby shales of the Earn Group.

Acknowledgements

The authors thank Bonnie C. Pemberton for preparation of the electron-microprobe mounts and for help with the SEM study. The manuscript was improved by comments from Richard Taylor, Dan Kontak, Robert Martin and Pavel Alexandrov. The claim owner, Ron Berdahl, is thanked for access to the property and information that was vital for this study. Financial support was provided by the Natural Sciences and Engineering Research Council of Canada in the form of Research Grants to LAG and DDM. Inconnu Lodge and True North Gems provided logistical and helicopter support. The C.S. Lord Geoscience Centre, NWT, is thanked for financial and field support.

References

Bakker, R.J. (1999): Adaptation of the Bowers and Helgeson (1983) equation of state for the H_2O–CO_2–CH_4–N_2–NaCl system. *Chem. Geol.* **154**, 225-236.

Banks, D.A., Giuliani, G., Yardley, B.W.D. & Cheilletz, A. (2000): Emerald mineralization in Columbia: fluid chemistry and the role of brine mixing. *Mineral. Deposita* **35**, 699-713.

Beus, A.A. & Mineev, D.A. (1972): Some geological and geochemical features of the emerald-bearing Muzo–Coscuez emerald zone, Cordillera Oriental, Columbia. *Geol. Rudn. Mestorozhd.* **16**, 18-30 (in Russ.).

Blusson, S.L., Green, L.H. & Roddick, J.A. (1968): Geology, Nahanni, District of Mackenzie and Yukon Territory; *Geol. Surv. Can., Map* **8–1967**.

Bowers, T.S. & Helgeson, H.C. (1983): Calculation of the thermodynamic and geochemical consequences of nonideal mixing in the system H_2O–CO_2–NaCl on phase relations in geologic systems: equation of state for H_2O–CO_2–NaCl fluids at high pressures and temperatures. *Geochim. Cosmochim. Acta* **47**, 1247-1275.

BOWMAN, J.R., COVERT, J.J., CLARK, A.H. & MATHIESON, G.A. (1985): The Cantung E zone scheelite skarn orebody, Tungsten, Northwest Territories: oxygen, hydrogen and carbon isotope studies. *Econ. Geol.* **80**, 1872-1895.

BROWN, P.E. (1989): FLINCOR. A microcomputer program for reduction and investigation of fluid inclusion data. *Am. Mineral.* **74**, 1390-1393.

CESARE, B., MARCHESI, C., HERMANN, J. & GÓMEZ-PUGNAIRE, M.T. (2003): Primary melt inclusions in andalusite from anatectic graphitic metapelites: implications for the position of the Al_2SiO_5 triple point. *Geology* **31**, 573–576.

CHEN, Z., WEIDNER, D.J., VAUGHAN, M.T., LI, R., PARISE, J.B., KOLEDA, C.C., BALDWIN, K.J. & LIEBERMANN, R.C. (1997): New developments at NSLS–X17B1 for *in situ* X-ray diffraction at high P–T; time-resolved diffraction measurement with and without imaging plate. *Trans. Am. Geophys. Union* (*Eos*) **78**, 775 (abstr.).

CLAYTON, R.N. & MAYEDA, T.K. (1963): The use of bromine pentafluoride in the extraction of oxygen from oxides and silicates for isotopic analysis. *Geochim. Cosmochim. Acta* **27**, 43-52.

DAWSON, K.M. & DICK, L.A. (1978): Regional metallogeny of the northern Cordillera, tungsten and base metal-bearing skarns in southeastern Yukon and southwestern Mackenzie. *Geol. Surv. Can., Pap.* **78–1A**, 287-292.

DHAMELINCOURT, P., BENY, J., DUBESSY, J. & POTY, B. (1979): Analyse d'inclusions fluides à la microsonde Mole à effet Raman. *Bull. Minéral.* **102**, 600-610.

DIAMOND, L.W. (1992): Gas clathrate hydrates in fluid inclusions: phase equilibria and applications. *Fourth Biennial Pan-American Conference on Research on Fluid Inclusions* (*PACROFI IV*), *Program Abstr.*, 119-122.

________ (2001): Review of the systematics of CO_2–H_2O fluid inclusions. *Lithos* **55**, 69-99.

GIULIANI, G., FRANCE-LANORD, C., COGET, P., SCHWARZ, D., CHEILLETZ, A., BRANQUET, Y., GIARD, D., MARTIN-IZARD, A., ALEXANDROV, P. & PIAT, D.H. (1998): Oxygen isotope systematics of emerald: relevance for its origin and geological significance. *Mineral. Deposita* **33**, 513-519.

GLOVER, J.K. & BURSON, M.J. (1987): Geology of the Lened tungsten skarn deposit, Logan Mountains, Northwest Territories. *Can. Inst. Mining Metall., Spec. Vol.* **37**, 255-265.

GORDEY, S.P. & ANDERSON, R.G. (1993): Evolution of the northern Cordilleran miogeocline, Nahanni map area (105I), Yukon and Northwest Territories. *Geol. Surv. Can., Mem.* **428**.

________ & MAKEPEACE, A.J., compilers (1999): Yukon digital geology. *Geol. Surv. Can., Open File* **D3826**.

GRAZIANI, G., GÜBELIN, E. & LUCCHESI, S. (1983): The genesis of an emerald from the Kitwe District, Zambia. *Neues Jahrb. Mineral., Monatsh.*, 175-186.

GREEN, L.H. & RODDICK, J.A. (1961): Geology, Nahanni, Yukon Territory and District of Mackenzie. *Geol. Surv. Can., Map* **14–1961**.

GROAT, L.A., MARSHALL, D.D., GIULIANI, G., MURPHY, D.C., PIERCEY, S.J., JAMBOR, J.L., MORTENSEN, J.K., ERCIT, T.S., GAULT, R.A., MATTEY, D.P., SCHWARZ, D., MALUSKI, H., WISE, M.A., WENGZYNOWSKI, W. & EATON, W.D. (2002): Mineralogical and geochemical study of the Regal Ridge showing emeralds, southeastern Yukon. *Can. Mineral.* **40**, 1313-1338.

GRUNDMANN, G. & MORTEANI, G. (1989): Emerald mineralisation during regional metamorphism: the Habachtal (Austria) and Leydsdorp (Transvaal, South Africa) deposits. *Econ. Geol.* **84**, 1835-1849.

GÜBELIN, E.J. (1958): Emeralds from Sandawana. *J. Gemmology* **6**, 340-354.

HAMMARSTROM, J.M. (1989): Mineral chemistry of emeralds and some associated minerals from Pakistan and Afghanistan: an electron microprobe study. *In* Emeralds of Pakistan: *Geology*, *Gemology and Genesis* (A.H. Kazmi & L.W. Snee, eds.). Van Nostrand Reinhold Company, New York, N.Y. (125-150).

HANNI, H.A. & KLEIN, H.H. (1982): Ein Smaragdvorkommen in Madagaskar. *Z. Deutsch. Gemmol. Gesellsch.* **21**, 71-77.

HICKMAN, A.C.J. (1972): The Miku emerald deposit. *Geol. Surv. Zambia, Econ. Rep.* **27**.

HOLDAWAY, M.J. (1971): Stability of andalusite and the aluminum silicate phase diagram. *Am. J. Sci.* **271**, 97-131.

KELLY, W.C. & BURGIO, P.A. (1983): Cryogenic scanning electron microscopy of fluid inclusions in ore and gangue minerals. *Econ. Geol.* **78**, 1262-1267.

KOVALOFF, P. (1928): Geologist's report on Somerset emeralds. *S. Afr. Mining Engineer. J.* **39**, 101-103.

KOZLOWSKI, A., METZ, P. & ESTRADA JARAMILLO, H.A.E. (1988): Emeralds from Somondoco, Columbia: chemical composition, fluid inclusions and origin. *Neues Jahrb. Mineral., Abh.* **159**, 23-49.

LEITMEIER, H. (1937): Das Smaragdvorkommen in Habachtal in Salzburg und seine Mineralien. *Tschermaks Mineral. Petrogr. Mitt.* **49**, 245-368.

MARSHALL, D., GROAT, L., GIULIANI, G., MURPHY, D., MATTEY, D., ERCIT, T.S., GAULT, R.A., WISE, M.A., WENGZYNOWSKI, W. & EATON, W.D. (2003): Pressure, temperature and fluid conditions during emerald precipitation, southeastern Yukon, Canada: fluid inclusion and stable isotope evidence. *Chem. Geol.* **194**, 187-199.

________, PEMBERTON, B.C., GROAT, L.A., VOORMEIJ, D. & MULJA, T. (2002): Fluid inclusions from the Little Nahanni Sn–Ta–Nb pegmatite complex, Northwest Territories. *Eighth Biennial Pan-American Conference on Research on Fluid Inclusions* (*PACROFI VIII*), *Program Abstr.*, 62-63.

MARTIN, H.J. (1962): Some observations on southern Rhodesian emeralds and chrysoberyls. *J. Chamber of Mines* **4**, 34-38.

MATHIESON, G.A. & CLARK, A.H. (1984): The Cantung E Zone scheelite skarn orebody, Tungsten, Northwest Territories: a revised genetic model. *Econ. Geol.* **79**, 883-901.

OTERO MUÑOZ, G. & BARRIGA VILLALBA, A.M. (1948): *Esmeraldas de Columbia.* Banco de la Republica, Bogota, Colombia.

OTTAWAY, T.L. (1991): *The Geochemistry of the Muzo Emerald Deposit, Columbia.* M.Sc. thesis, Univ. Toronto, Toronto, Ontario.

________, WICKS, F.J., BRYNDZIA, L.T., KYSER, T.K. & SPOONER, E.T.C. (1994): Formation of the Muzo hydrothermal emerald deposit in Columbia. *Nature* **369**, 552-554.

PETRUSENKO, S., ARNAUDOV, V. & KOSTOV, I. (1966): Emerald pegmatite from the Urdini Lakes, Rila Mountains. *Annuaire de l'Université de Sofia, Faculté de Géologie et Géographie* **59**, 247-268 (in Bulg.).

POUCHOU, J.L. & PICHOIR, F. (1991): Quantitative analysis of homogeneous or stratified microvolumes applying the model "PAP". *In* Electron Probe Quantitation (K.F.J. Heinrich & D.E. Newbury, eds.). Plenum Press, New York, N.Y. (31-75).

ROEDDER, E. (1984): Fluid Inclusions. *Rev. Mineral.* **12**.

SCHWARZ, D. & GIULIANI, G. (2001): Emerald deposits – a review. *Aust. Gemmol.* **21**, 17-23.

SHEPPARD, S.M.F. (1986): Characterization and isotopic variations in natural waters. *In* Stable Isotopes in High Temperature Geological Processes (J.W. Valley, H.P. Taylor Jr. & J.R. O'Neil, eds.). *Rev. Mineral.* **16**, 165-183.

SINKANKAS, J. (1981): *Emeralds and other Beryls*. Chilton Book Co., Radnor, Pennsylvania.

VAPNIK, Y. & MOROZ, I. (2000): Fluid inclusions in emerald from the Jos complex (central Nigeria). *Schweiz. Mineral. Petrogr. Mitt.* **80**, 117-129.

VLASOV, K.A. & KUTAKOVA, E.I. (1960): *Izumrudnye Kopi.* Akad. Nauk SSSR, Moscow, Russia.

WALTON, L. (1997): *Geological Report for assessment requirements, Lened Property, NWT.*

ZAMBONINI, F. & CAGLIOTO, V. (1928): Ricerche chimiche sulla rosterite di San Piero in Campo (Isola d'Elba) e sui berilli in generale. *Gazz. Chim. Ital.* **58**, 131-152.

ZHANG, YI-GANG & FRANTZ, J.D. (1987): Determination of the homogenisation temperatures and densities of supercritical fluids in the system NaCl–KCl–$CaCl_2$–H_2O using synthetic fluid inclusions. *Chem. Geol.* **64**, 335-350.

Received November 15, 2002, revised manuscript accepted March 28, 2004.

APPENDIX: ANALYTICAL PROCEDURES

Electron-microprobe analyses of emerald from Lened were made with a fully automated Cameca SX–50 instrument operating in wavelength-dispersion mode at the University of British Columbia. Operating conditions were as follows: voltage 15 kV, beam current 20 nA, and beam diameter 30 μm. Data for standards were collected for 50 s, and data for samples were collected for 50 s for all elements except Al (30 s) and Si (20 s). For analyses of emerald, the following standards were used: albite (Na, Al, Si), diopside (Mg, Ca), orthoclase (K), rutile (Ti), scandium (Sc), vanadium (V), magnesiochromite (Cr), synthetic fayalite (Fe), synthetic rhodonite (Mn), and pollucite (Cs). The $K\alpha$ lines were used for all elements except Cs ($L\alpha$), and Ti was sought but not detected. Data reduction was done using the PAP method (Pouchou & Pichoir 1991). Scandium, V, Cr, and Cs values for emerald were reported as both oxide wt.% and ppm, with the ppm values obtained from the laser-ablation microprobe technique.

A Merchantek UV laser-ablation microprobe (LAM) coupled to a VG PQIIS + Inductively Coupled Plasma – Mass Spectrometer (ICP–MS) at the University of Victoria was used to measure trace-element concentrations in the emerald samples. The pit size of the LAM was approximately 50 μm. The calibration standard was NIST 613 synthetic silicate, and SRM BCR–2 (Columbia River Basalt) was used as a quality-control standard. Major- and trace-element contents of the standards, determined by ICP–MS, are given in Chen *et al.* (1997). An SiO_2 value of 65.0 wt.% in beryl was used to standardize the LAM–ICP–MS data for the Lened samples.

Fluid-inclusion microthermometric measurements were made on doubly polished chips of quartz and emerald. Phase changes within these samples were observed using a modified Linkam THMSG–600 heating–freezing stage fitted to an Olympus BX50 microscope at Simon Fraser University. The stage was calibrated with two synthetic fluid inclusion standards. One composed of pure H_2O was used to calibrate the stage at 0° and 374.1°C. The second standard, containing H_2O and CO_2, was used to calibrate the stage at –56.6°C. The temperatures of the phase transitions within the fluid inclusion standards was periodically checked, and the error was invariably within 0.1°C of the two low-temperature calibration points and within 1.0°C of the higher-temperature calibration point. Preliminary isotopic analyses of the structurally bound oxygen in emerald from the Lened occurrence were carried out at the Centre de Recherche Pétrographiques et Géochimiques (CRPG) in Nancy, France. The modified technique of Clayton & Mayeda (1963) is described in Giuliani *et al.* (1998). Limited sample material precluded the analysis of channel H_2O within emerald, as was done by Groat *et al.* (2002) for the Regal Ridge showing.